

Solid State Transitions in Alkali Alkanoates: Diffractometric and Conductometric Measurements on Rubidium and Cesium Propanoates

G. Spinolo, A. Cingolani, and M. Sanesi

Centro di Studio per la Termodinamica ed Elettrochimica dei Sistemi Salini Fusi
e Solidi del C.N.R.
c/o Istituto di Chimica Fisica e di Elettrochimica della Università, Pavia, Italy

Z. Naturforsch. **34a**, 1212—1215(1979); received August 2, 1979

Conductometric measurements on solid rubidium and cesium propanoates and X-ray powder diffraction measurements on the rubidium salt have been carried out over suitable temperature ranges. The results obtained, along with the previous ones concerning the lithium, sodium and potassium salts, have been discussed in relation to possible melting mechanisms (involving various kinds of disorder, e.g., positional, orientational, conformational) active in the alkali alkanoates family.

1. Introduction

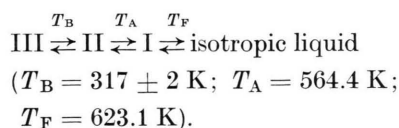
The present work aims at giving a contribution to the knowledge of the stepwise melting process in the alkali alkanoates family. To this purpose, the X-ray powder diffraction and conductance measurements, carried out previously [1] on a number of solid phases of lithium, sodium and potassium propanoates, are now extended to the rubidium and cesium salts. The information thus obtained satisfactorily supplements the interpretation of the fusion mechanism, already suggested by other authors for higher homologues.

2. Experimental and Results

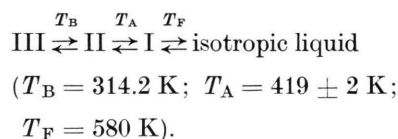
2.1. The procedure followed for preparing and handling the salts [2] and for performing the polythermal conductance and X-ray powder diffraction measurements [1] were described previously.

The phase relationships were stated through DSC analysis [2] as follows:

a) *Rubidium propanoate*:



b) *Cesium propanoate*:



where T_A and T_B refer to solid state transitions (sstr) A and B, respectively.

2.2. For both salts the conductance measurements covered the temperature range from $(T_A - 50)$ to $(T_A + 50)$, whereas the region around T_B could not be explored for instrumental reasons. The derivative plots, $d \log G/dT$ vs. T , are compared with the pertinent DSC data in Figure 1, while the strictly linear dependence of $\log G$ on $1/T$ is shown in Figure 2. The relevant E_∞ 's (practically coincident with the corresponding E_G 's, see [1]) are summarized in Table 1 together with the α_{tr} data (as obtained at T_A by extrapolation), the latter estimated in an approximate way from the dimensions of the pellet-shaped cells. The activation energy, as expected, decreases going from phase II (stable at lower temperature) to phase I (stable at higher temperature).

2.3. In the series from sodium to cesium propanoates the increase of the cation size causes the hygroscopicity to increase and the thermal stability of the higher temperature phase to decrease: satisfactory X-ray diffraction patterns could still be obtained with rubidium propanoate, whereas the less reliable ones taken on the cesium salt will not be discussed here.

Reprint requests to Prof. M. Sanesi, Istituto di Chimica Fisica e di Elettrochimica dell'Università, Viale Taramelli, 16, I-27100 Pavia (Italy).

0340-4811 / 79 / 1000-1212 \$ 01.00/0. — Please order a reprint rather than making your own copy.



Dieses Werk wurde im Jahr 2013 vom Verlag Zeitschrift für Naturforschung in Zusammenarbeit mit der Max-Planck-Gesellschaft zur Förderung der Wissenschaften e.V. digitalisiert und unter folgender Lizenz veröffentlicht: Creative Commons Namensnennung-Keine Bearbeitung 3.0 Deutschland Lizenz.

Zum 01.01.2015 ist eine Anpassung der Lizenzbedingungen (Entfall der Creative Commons Lizenzbedingung „Keine Bearbeitung“) beabsichtigt, um eine Nachnutzung auch im Rahmen zukünftiger wissenschaftlicher Nutzungsformen zu ermöglichen.

This work has been digitalized and published in 2013 by Verlag Zeitschrift für Naturforschung in cooperation with the Max Planck Society for the Advancement of Science under a Creative Commons Attribution-NoDerivs 3.0 Germany License.

On 01.01.2015 it is planned to change the License Conditions (the removal of the Creative Commons License condition "no derivative works"). This is to allow reuse in the area of future scientific usage.

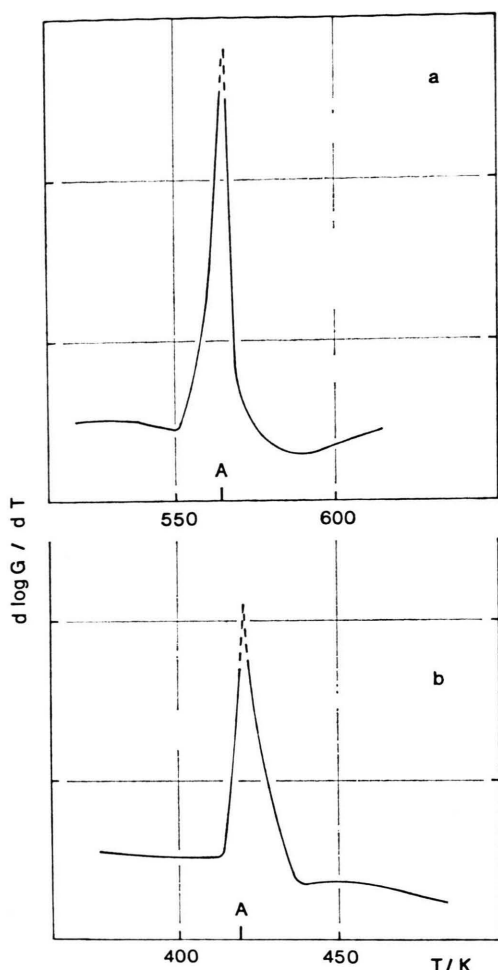


Fig. 1. Conductometric detection of the sstr temperatures in rubidium (a) and cesium (b) propanoates (ordinates in arbitrary units). The DSC values are indicated by vertical lines on the abscissa.

Table 1. Electrical conductance parameters for rubidium and cesium propanoate solid phases.

Salt	Phase	Temperature range [K]	κ_{tr} [$S\ m^{-1}$]	E_{κ} [$kJ\ mol^{-1}$]
Rubidium propanoate	I	610–564	$2 \cdot 10^{-3}$	106 ± 2
	II	564–510	$4 \cdot 10^{-4}$	135 ± 2
Cesium propanoate	I	470–419	$8 \cdot 10^{-5}$	62 ± 4
	II	419–370	$3 \cdot 10^{-5}$	70 ± 4

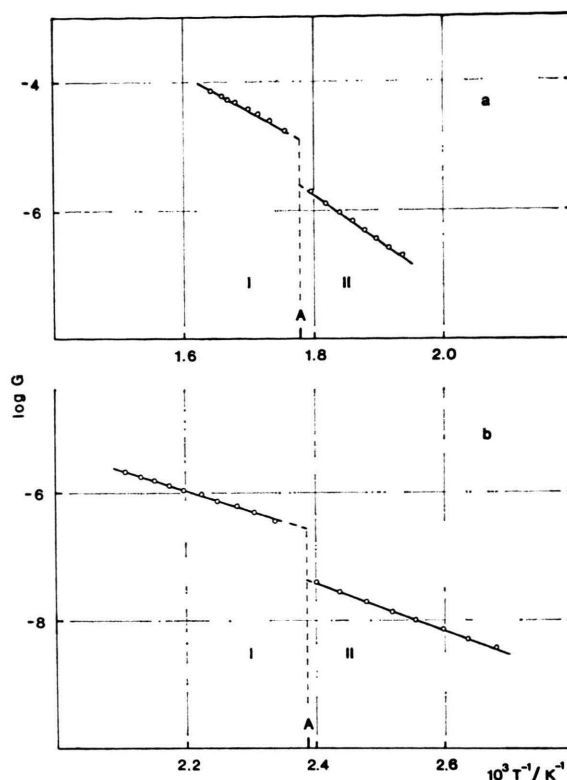


Fig. 2. Dependence of $\log G$ vs. $1/T$ in the temperature range from $(T_A - 50)$ to $(T_A + 50)$ for rubidium (a) and cesium (b) propanoates (points read out from recorded curves G/S vs. T/K).

Concerning rubidium propanoate, measurements were performed between room temperature and 585 K. The best data were obtained for phase II, which was indexed as an orthorhombic unit cell containing two molecules. Diffraction patterns taken at 570–585 K on phase I looked rather similar, although exhibiting a number of extra lines most likely due to decomposition products*. Reliable diffractograms of phase III could be obtained only after the material was submitted to prolonged dehydration at $T > T_B$ within the polythermal chamber. Although not indexed, they looked to some extent analogous to those taken on phase III of potassium propanoate, and apparently exhibited the reflections corresponding to the lines (00 l) of higher temperature phases.

The trend of the lattice parameters is shown in Fig. 3 for phases I and II.

* At a given temperature the intensity of these lines increased with time.

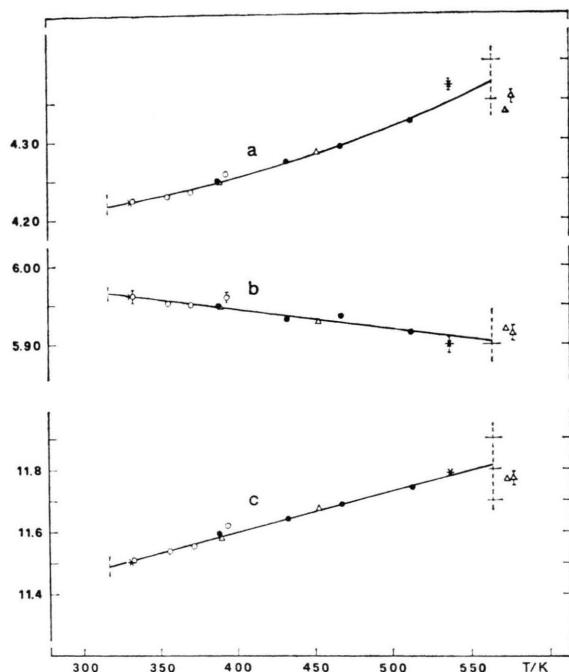


Fig. 3. Temperature dependence of the lattice parameters in phase I and II of rubidium propanoate (different symbols refer to different samples). For phase II the smoothed values at 320, 400, 500 and 560 K are the following: $a/\text{\AA} = 4.217, 4.251, 4.317, 4.369$; $b/\text{\AA} = 5.965, 5.945, 5.920, 5.905$; $c/\text{\AA} = 11.492, 11.599, 11.733, 11.813$.

3. Discussion

3.1. Concerning the fusion process Ubbelohde and coworkers [3] suggested as possible also for alkali alkanoates: (i) a melting mechanism referable to positional disorder, which implies the "fusion" of a single sublattice (in this case the cationic one) and was already accepted for salts (e.g., AgI) where the ions are far different in size and the larger one is highly polarizable; (ii) a melting mechanism referable to orientational disorder, which implies the ability for a given kind of structural unit to assume several orientations within the lattice.

On the other hand, from the X-ray results obtained by Skoulios and Luzzati [4], and by Gallot and Skoulios [5] on several medium- and long-chain alkanoates, a distinction can be made between melting of the hydrocarbon chains and fusion of the bidimensional ionic lattice. The former process should be bound to roto-vibrational degrees of freedom, the activation of which causes the anion to assume a quasispherical shape at higher temperatures, whereas at lower temperatures the

chains are frozen in a fixed conformation. The latter one, in turn, might occur by steps, each involving a particular intermediate structure (ribbons, discs, etc.).

3.2. From our previous [1] and present results on propanoates, it can be reasonably assumed that the lattice constants a and b define the rectangular net of the (double-layered) packing of the anion polar ends and of the alkali counterions, while constant c regards the tail-to-tail packing of the aliphatic chains. This assumption, being consistent with the structural evidence gained by Lomer and coworkers [6] on potassium butanoate and a few even higher homologues, allows to justify through simple geometrical considerations (taking into account, *inter alia*, the variation of the cationic radii) the changes experimentally observed for the a and b values in the sequence of sodium, potassium and rubidium propanoates.

It is also worthwhile mentioning that in the latter salts the coexistence of strong ionic interactions (mainly active in the ab plane) and weak Van der Waals interactions (mainly active in the space between the ab planes, i.e., along the c direction) reflects on the magnitude of the thermal expansion coefficients, α . Indeed, for the propanoates in the temperature range explored it was found $\frac{1}{2}\alpha_{ab} = 40\text{--}60 \cdot 10^{-6} \text{ K}^{-1}$ and $\alpha_c = 100\text{--}160 \cdot 10^{-6} \text{ K}^{-1}$; these values may be compared with the linear expansion coefficient (at room temperature) of an ionic solid (e.g., NaCl: $40 \cdot 10^{-6} \text{ K}^{-1}$) and of paraffin ($110 \cdot 10^{-6} \text{ K}^{-1}$), respectively.

For what in particular concerns the temperature dependence of the lattice constant b , it is still to be stressed that α_b turns from slightly positive in the case of the sodium salt to negative in the case of the larger cations. The observed anomaly might be due to some kind of orientational disorder, such as rotation of the carboxylic groups in the ionic planes: this possibility should increase with increasing cationic size and is expected to affect significantly the thermal expansion, owing to the high character of anharmonicity of the corresponding degree of freedom. Finally, the conductometric results, i.e., low specific conductivity and high activation energies, suggest that a mechanism of (cationic) positional disorder is not effective in the alkali propanoates.

3.3. As a conclusion, it appears that the measurements on the alkali propanoates are useful for

getting additional information on the roles played by the melting mechanisms, possibly active in the alkanoates family and respectively bound to positional, orientational and conformational disorder.

It may be stressed that the short chain-length makes the propanoates particularly suitable to evidence the contribution of orientational disorder, which can be more or less masked by the other effects in higher homologues. In fact, when the

chain-length increases, the contribution of the conformational disorder becomes more and more remarkable. Thermal activation of the pertinent degrees of freedom causes in the anions a change in shape progressively approaching the spherical one: thus, the conditions may be reached also for positional disorder (in the cationic sublattice) to take place. Should this occur, mesomorphic phases characterized with high ionic mobility may form.

- [1] A. Cingolani, G. Spinolo, and M. Sanesi, *Z. Naturforsch.* **34a**, 575 (1979).
- [2] P. Ferloni, M. Sanesi, and P. Franzosini, *Z. Naturforsch.* **30a**, 1447 (1975).
- [3] (a) J. J. Duruz, H. J. Michels, and A. R. Ubbelohde, *Proc. Roy. Soc. London* **322** A, 281 (1971); (b) A. R. Ubbelohde, *Melting and Crystal Structure*, Clarendon Press, Oxford 1965.
- [4] (a) A. Skoulios and V. Luzzati, *Nature London* **183**, 1310 (1959); (b) A. Skoulios and V. Luzzati, *Acta Cryst.* **14**, 278 (1961).
- [5] B. Gallot and A. Skoulios, *Koll.-Z. Polym.* **209**, 164 (1966); **210**, 143 (1966); **213**, 143 (1966); *Mol. Crystals* **1**, 263 (1966).
- [6] (a) V. Vand, T. R. Lomer, and A. Lang, *Acta Cryst.* **2**, 214 (1949); (b) T. R. Lomer, *Acta Cryst.* **5**, 11, 14 (1952); (c) J. H. Dumbleton and T. R. Lomer, *Acta Cryst.* **19**, 301 (1965).